This article has been accepted for publication in a future issue of this journal, but has not been fully edited. Content may change prior to final publication. Citation information: DOI 10.1109/TNSRE.2014.2365697, IEEE Transactions on Neural Systems and Rehabilitation Engineering

Design and Control of the *MINDWALKER* Exoskeleton

Shiqian Wang*, Letian Wang*, Cory Meijneke, Edwin van Asseldonk, Thomas Hoellinger, Guy Cheron, Yuri Ivanenko, Valentina La Scaleia, Francesca Sylos-Labini, Marco Molinari, Federica Tamburella, Iolanda Pisotta, Freygardur Thorsteinsson, Michel Ilzkovitz, Jeremi Gancet, Yashodhan Nevatia, Ralf Hauffe, Frank Zanow, and Herman van der Kooij

***Abstract*—Powered exoskeletons can empower paraplegics to stand and walk. Actively controlled hip ab/adduction (HAA) is needed for weight shift and for lateral foot placement to support dynamic balance control and to counteract disturbances in the frontal plane. Here, we describe the design, control, and preliminary evaluation of a novel exoskeleton, *MINDWALKER*. Besides powered hip flexion/ extension and knee flexion/extension, it also has powered HAA. Each of the powered joints has a series elastic actuator, which can deliver 100Nm torque and 1kW power. A finite-state machine based controller provides gait assistance in both the sagittal and frontal planes. State transitions, such as stepping, can be triggered by the displacement of the Center of Mass (CoM). A novel step-width adaptation algorithm was proposed to stabilize lateral balance. We tested this exoskeleton on both healthy subjects and paraplegics. Experimental results showed that all users could successfully trigger steps by CoM displacement. The step-width adaptation algorithm could actively counteract disturbances, such as pushes. With the current implementations, stable walking without crutches has been achieved for healthy subjects but not yet for SCI paraplegics. More research and development is needed to improve the gait stability.**

***Index Terms*—*MINDWALKER*, exoskeleton, SEA, XCoM, gait assistance, balance control**

Manuscript received November 05, 2013; revised August 21, 2014; accepted October 19, 2014. Date of Publication November XX, 2014; date of current version November XX 2014. This work was supported by EU FP7 Programme under contract #247959. *MINDWALKER* was the project title and the name of the exoskeleton. In short, the goal of the project was to create a *mind*-controlled orthosis to help paraplegics *walk*.

* Authors have equal contribution to this paper.

S. Wang and C. Meijneke are with Biomechanical Engineering., Delft University of Technology, 2628CD Delft, the Netherlands (phone: +31 152788634; e-mail: shiqian.wang@tudelft.nl; C.Meijneke@tudelft.nl).

L. Wang and E. van Asseldonk are with Biomechanical Engineering, University of Twente, 7522NB Enschede, the Netherlands (e-mail: letian.wang@utwente.nl; E.H.F.vanAsseldonk@utwente.nl).

T. Hoellinger and G. Cheron are with Laboratory of Neurophysiology & Movement Biomechanics, Université Libre de Bruxelles, 1070 Brussels, Belgium (e-mail: hoellint@gmail.com; gcheron@ulb.ac.be).

Y. Ivanenko, V. La Scaleia, and F. Sylos-Labini are with Dept. of Neuromotor Physiology, IRCCS Fondazione Santa Lucia, 00179 Rome, Italy. V. La Scaleia and F. Sylos-Labini are also with Dept. of Systems Medicine, University of Rome Tor Vergata, 00133 Rome, Italy. (e-mail: y.ivanenko@hsantalucia.it; v.lascaleia@hsantalucia.it; f.syloslabini@hsantalucia.it).

M. Molinari, F. Tamburella, and I. Pisotta are with Neurorehab. Clinical Unit A and Experimental Neurorehab. Lab, IRCCS Fondazione Santa Lucia, 00179 Rome, Italy (e-mail: m.molinari@hsantalucia.it; f.tamburella@ hsantalucia.it; i.pisotta@hsantalucia.it).

F. Thorsteinsson is with OSSUR, 110 Reykjavík, Iceland (e-mail: fthorsteinsson@ossur.com).

M. Ilzkovitz, J. Gancent and Y. Nevatia are with Space Applications Services N.V./S.A., 1932 Zaventem, Belgium (e-mail: michel.ilzkovitz@gmail.com; jeremi.gancet@spaceapplications.com; yashodhan.nevatia@spaceapplications.com).

R. Hauffe is with eemagine Medical Imaging Solutions GmbH, 10243 Berlin, Germany (e-mail: Ralf.Hauffe@eemagine.com)

F. Zanow is with ANT Neuro, 7521PT Enschede, the Netherlands (e-mail: frank.zanow@eemagine.com).

H. van der Kooij is with Biomechanical Engineering, University of Twente, 7522NB Enschede, The Netherlands. He is also with Biomechanical Engineering, Delft University of Technology, 2628CD Delft, the Netherlands (e-mail: H.vanderKooij@utwente.nl).

I. Introduction

Spinal cord injury (SCI) has high personal impacts and socio-economic consequences. Patients with SCI place a heavy burden on the health-care system [1]. The prevalence of SCI in Northern America, Australia, and Europe is estimated to be between 223 and 755 per million populations; and the incidence of SCI lies between 10.4 and 83 per million inhabitants per year worldwide [2]. Two thirds of SCI patients are estimated to be paraplegic; most patients with SCI are young men in their thirties, who need to work to support their families [1]. They have to rely on help from the health-care system and social security system. In a survey [3], 59 percent of paraplegics rated the *restoration of walking* as their first or second priority for improvement in quality of life.

Orthotic devices have been developed to provide paraplegics with some degree of locomotion capability and to reduce the occurrences of secondary complications. Passive (unpowered) orthoses are often prescribed. However, due to the passive nature of these devices, the metabolic energy expenditure in gait causes frequent abandonment or low utilization [4]-[6]. Seeing the limitations of passive orthoses, researchers started developing active exoskeletons as early as the 1960s [7]. However, rapid developments have only been achieved in recent years, resulting in several wearable exoskeletons [8]-[19]. Several of these devices are specifically designed to restore walking for SCI subjects [10]-[19].

Despite the impressive progress and promising results, there is a need to improve the technology. Although SCI patients are enabled to walk again, for stability they rely on crutches, and their walking pattern is less fluent and slower than natural human gait.

This article has been accepted for publication in a future issue of this journal, but has not been fully edited. Content may change prior to final publication. Citation information: DOI 10.1109/TNSRE.2014.2365697, IEEE Transactions on Neural Systems and Rehabilitation Engineering

We believe that powered hip ab/adduction (HAA) is necessary for balance in bipedal gait. Mathematical modeling has shown that passive bipedal walking is laterally unstable, even though it retains stability in the sagittal plane [20][21]. Foot placement (step-width adaptation) can effectively stabilize lateral balance in passive walking [21]-[24]. Human experiments demonstrate that foot placement is actively controlled because a loss of sensory information results in less precise foot placement [23]. As paraplegics have lost or impaired control of their legs, self-balanced walking of paraplegics wearing an exoskeleton requires powered HAA. To make use of the powered HAA, an online step-width adaptation (SWA) algorithm is presented in this paper, in an attempt to improve gait stability. The algorithm is based on the "extrapolated center of mass" (XCoM) concept, which has been successfully applied in analyzing human balance control [24][25]. XCoM is a spatial variable used to formulate a stability condition, which is valid in both static and dynamic situations [26].

In terms of actuation, force-controllable actuators are desired. These allow different control implementations, e.g. force control, bio-inspired control, and impedance control [27]. The latter can be used to regulate the joint/leg impedance. In humans, adaptive control of mechanical impedance has been shown to be necessary for manipulation and locomotion [28]. There is more than one way to achieve force control, such as using load cells or motor current regulation. In the current design, series elastic actuation (SEA) was chosen, because it has benefits, such as low output impedance, backdrivability, increased force fidelity, added safety, etc., as pointed out by others [29]. Additionally, similar to the function of tendons connected to biological muscles, the series spring can potentially store energy, increase efficiency, and filter shock loads. Currently few exoskeletons have used SEA in their design (see e.g. [16] and [19]).

The goal of this research is to develop a powered exoskeleton to support SCI paraplegics to walk. The exoskeleton is named *MINDWALKER* (*MW* for short). *MW* is equipped with series elastic actuators (SEAs), and that allows exploring different control implementations and safe and compliant interactions with its surroundings. This exoskeleton is capable of performing two-dimensional foot placement over ground thanks to the actuated HAA. We have developed algorithms to determine the user-intended motion, to assist weight shift, and to online adapt the step width to maintain balance.

In this paper, the design requirements are specified first, followed by the exoskeleton hardware description in section III. The control and human machine interface (HMI) implementations are presented in section IV. The experimental results and discussion are given in section V and VI.

II. Design Requirements of a Lower Limb Exoskeleton

The aim is to develop a research prototype that can empower lower limb disabled people (especially SCI patients) to walk on level-ground, and maintain postural stability. The target maximal walking speed is 0.8m/s. *MW* is supposed to be able to accommodate the anatomical measures of 90 percent of the European adult population, which dictates the wearer height and hip width. These values are retrieved from the DINED database (http://dined.nl/), by taking the 5 and 95 percentile numbers. The exoskeleton weight is required to be less than 30 kg, based on the weight of existing exoskeletons (*Ekso* [12] and *ReWalk* [10] are 20~25kg and *REX* [17] 38kg). The basic technical requirements are briefly summarized in Table I.

Based on human anatomy and joint range of motion (RoM), the desired DoFs and joint RoM for the exoskeleton are specified to allow sitting, standing, and walking (see Table II). Note that in the requirements, the knee extension is limited to 1.5 degree, to prevent hyperextension, in case misalignments between the exoskeleton and the wearer exist.

In order to support the wearer to maintain balance in both sagittal and frontal planes, hip ab/adduction, hip flexion/ extension (HFE) and knee flexion/extension (KFE) are required to be powered. Powered ankle dorsi/ plantarflexion (ADP) is also desired. However, this is a technical trade-off: On one hand, passive ADP can lead to a lightweight design and a lower inertia at the distal location [30]; on the other hand, powered ADP can provide active push-off, extra maneuverability, and balance capability. In this prototype, ADP is passive, in order to achieve a lightweight design. The hip endo/exo-rotation (HEE) and ankle inversion/eversion (AIE) should be compliant to reduce impact and improve wearing comfort, either using compliant structure or spring-loaded joints. Ankle endo/exo-rotation (AEE) is locked because the rotation of the leg is taken care by HEE.

We collected and analyzed human gait data to facilitate the design by providing information such as joint velocities, torques, and powers (see previous work in [31]). Based on this information, we specify the actuation requirements (Table III). The series spring stiffness requires some trade-offs. First, SEA is desired to be able to render the joint impedances of all human leg joints. For a SEA, it is only possible to render stiffness lower than the physical spring stiffness at the output. According to previous studies (e.g. [31][32]), the quasi-stiffness of human

TABLE I
Technical Requirements of Mindwalker Exoskeleton

#	Items	Desired value
E1	Powered DoFs	4 per leg
E2	Target maximal walking speed	0.8m/s
E3	Max. allowable wearer weight	100kg
E4	Allowable wearer height	153~188cm
E5	Allowable wearer hip width	Up to 44cm
E6	Exoskeleton weight	<30kg

If, in the actual design, a requirement is not met, it is shaded with grey color; if met, no shading. The same holds for Table II and III.

TABLE II
Joint Range of Motion

#	Joints and DoFs		Powered	Desired Range of Motion
R1	Hip	HAA	Required	19º abduction/ 22º adduction
R2		HFE	Required	110 º flexion/ 18 º extension
R3		HEE	No	±10 º rotation
R4	Knee	KFE	Required	120 º flexion/ 1.5 º extension
R5	Ankle	ADP	No	20 º dorsiflexion/ 20 º plantarflexion
R6		AIE	No	10 º inversion/ 10 º eversion
R7		AEE	No	Rigid

HAA = hip ab/adduction; HFE = hip flexion/extension, HEE = Hip endo/exo-rotation; KFE =knee flexion/extension, ADP = ankle dorsi/plantarflexion; AIE = Ankle Inversion/Eversion, AEE = Ankle endo/exo-rotation

This article has been accepted for publication in a future issue of this journal, but has not been fully edited. Content may change prior to final publication. Citation information: DOI 10.1109/TNSRE.2014.2365697, IEEE Transactions on Neural Systems and Rehabilitation Engineering

TABLE III
DESIGN REQUIREMENTS FOR EXOSKELETON ACTUATION

#	ITEMS	Desired value
A1	Peak torque	100 Nm
A2	Peak power	>150 W
A3	Series spring stiffness	800 Nm/rad
A4	Small torque bandwidth@2Nm	20 Hz
A5	Large torque bandwidth@100Nm	4 Hz
A6	Output torque resolution	1 Nm
A7	Closed-loop control update frequency	1000Hz
A8	Joint mass	As light as possible

joints remains below *800 Nm/rad* for walking at 0.8 m/s. On one hand, from a control point of view, higher spring stiffness is desired, in order to allow a higher closed-loop control bandwidth. On the other hand, as the spring is also used for torque measurement, higher stiffness means smaller deformations under the same load, which would require high-resolution encoders to reach reasonable torque resolution. So 800 Nm/rad is considered the most suitable stiffness value for this application.

III. DESIGN OF *MINDWALKER*

This section highlights some design aspects, mainly including the exoskeleton structure, the actuation system, human-exoskeleton physical interfaces, and finally the electronics hardware.

A. *Exoskeleton Structure and Frame*

In *MW*, most of the joints are aligned with human joints, e.g., HFE and HAA axes intersect at the human hip joint center (see Fig. 1). HEE is not aligned with the hip joint center. Instead, it is offset and placed between HAA and HFE. This misalignment does not introduce extra stresses to human joints because 1) only small rotations occur in HEE and 2) relative movements between human limbs and exoskeleton limbs are allowed as a consequence of the chosen physical attachments (see section III.C).

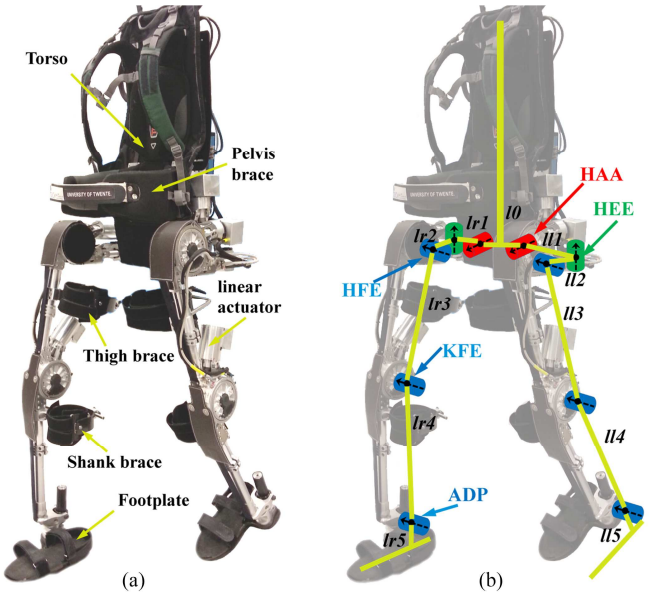

Fig. 1. *MW exoskeleton*. HAA and HFE axes intersect at the human hip joint center; KFE and ADP axes align with human knee and ankle joints, respectively. HAA, HFE, and KFE are powered; HEE and ADP are passive and spring loaded. Shank and thigh segments of the exoskeleton have telescopic tubular structure, which can accommodate subject height between 1.53 and 1.88m. Two HAAs are mounted on the pelvis structure (part of torso) using sliding rails, so that the exoskeleton can be adjusted to accommodate hip width up to 0.44m. Footplates are made of carbon fiber and have braces to attach human feet. Right below the knee, shank braces are used to support most of the weight of the user in standing and walking. Thigh braces are added to loosely constrain the upper leg and support the wearer during standing up. A pelvis brace and backpack braces are used to attach to the upper body of the wearer.

All DoFs are serially chained, in a sequence of HAA, HEE, HFE, KFE and ADP from pelvis to foot. This implies that the exoskeleton hip consists of three serially chained hinges, whereas the human hip has a ball-and-socket joint. The order of three hip rotations is determined based on three criteria: 1) as many of the three rotation axes as possible intersect at human hip joint centers; 2) no interference between exoskeleton parts and the human body in walking and sitting; 3) to minimize weight.

In the actual design HAA, HFE, and KFE are powered while HEE and ADP are passive and spring loaded. The ankle joint is equipped with antagonist spring pairs with its neutral position at 0º ankle angle. HEE is spring loaded. The springs are relatively stiff (equivalent joint stiffness is about 600 Nm/rad). AIE comes from the compliance in the carbon-fiber-rubber footplate.

As a research prototype, the exoskeleton has to be able to accommodate inter-subject anatomy diversities. Hence, a couple of adjustable mechanisms, such as telescopic structures in the thigh and shank, a sliding rail system in the pelvis, are created to fulfill E3-E5 design requirements (Table I).

B. *Series Elastic Joint - Actuation*

To accommodate the power and weight requirements, the actuation system, including power electronics and the actuators, was custom made (Fig. 2). For wearable devices, especially lower limb exoskeletons, the power-to-weight and torque-to-weight ratios of actuators have to be maximized to minimize the exoskeleton weight. Therefore, special efforts have been devoted to the actuation system design. The optimization of the actuation system has been given in [33]. A power-based quasi-static model of the SEA drivetrain has been built, and all the rotary joint quantities (joint torques and angles) were

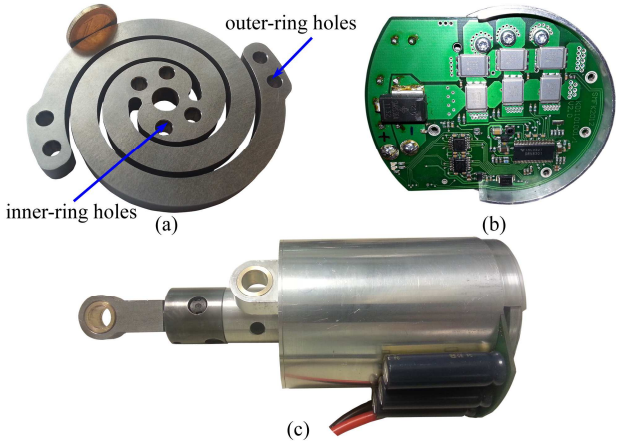

Fig. 2. *MW* actuation system. (a) photo of the double spiral series spring. Through those 4 inner-ring holes, 4 shoulder screws connect the inner ring to the leverarm; through those 4 outer-ring holes, 4 dowel pins connect the outer ring to the distal segment. See Fig. 3 as well. (b) drive electronics mounted at the back of the linear actuator; (c) linear actuator assembly

This article has been accepted for publication in a future issue of this journal, but has not been fully edited. Content may change prior to final publication. Citation information: DOI 10.1109/TNSRE.2014.2365697, IEEE Transactions on Neural Systems and Rehabilitation Engineering

converted step-by-step to the proper quantities at each component of the drivetrain (e.g., forces and linear velocities at the ballscrew, current at the motor). Using this model, we proposed an optimization framework to minimize the total mass of the battery, the ballscrew, and the motor. The properties of the actuation system are briefly summarized below.

The series spring is a torsional spring [33]-[35], specially developed to achieve the target stiffness while minimizing the weight. This spring has a double-spiral disc shape and is made of a single piece of high-grade titanium. It weighs 220g, has stiffness of 820 Nm/rad (2.5 percent off from the target value), and allows 100 Nm bidirectional torque loading. It exhibits 99.99 percent linearity in terms of load vs. deflection, which guarantees accurate joint torque sensing. The output end of the ballscrew is connected to the inner ring of the series spring via a leverarm (Fig. 3). The leverarm directly transforms the linear motion of the linear actuator to rotations of the inner ring of the torsional spring. The outer ring of the spring is connected to the distal segment.

The linear actuator consists of a ballscrew and an outrunner BLDC motor (Hacker A60 7S V2, Hacker Motor GmbH). The ballscrew (SKF SD 12X4) has a lead of 4mm and can handle more than 4000N axial force. It has 95 percent theoretical and above 90 percent practical mechanical efficiency, which makes the linear actuator backdrivable. No further reduction gear is used between the motor and ballscrew, since the motor can deliver 2.5Nm output torque and about 1kW power. It has relatively high motor constant, which introduces minimal copper losses for a given torque (see [33] for explanation). The drive electronics, mainly consisting of 6 Power MOSFETs (type IRF7749, International Rectifier, USA) and a gate driver (DRV8301, Texas Instruments Inc., USA), is integrated at the back of the actuator. The MOSFET has a low on-resistance (1.5mΩ at most) and therefore low switching losses. The motor commutation is controlled using a 12-bit absolute magnetic encoder (iC-MH8, iC-Haus GmbH). The same encoder is used for the velocity control of the motor.

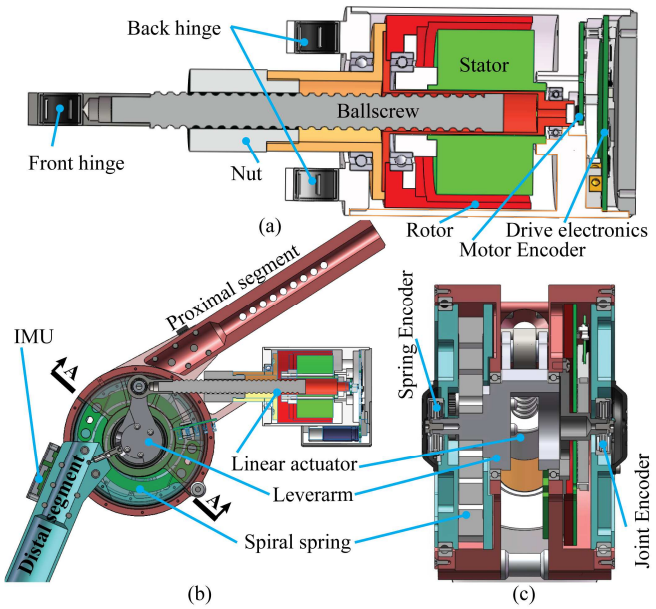

Fig. 3. CAD drawing of the *MW* actuation system. (a) the cross section of the linear actuator; (b) cross section (cut in the sagittal plane) of a series elastic joint; (c) the A-A cross section of (b)

The SEA consists of the linear actuator, the double-spiral spring, the spring deflection and joint encoders (17-bit resolution, Netzer DS-25, Netzer Precision Motion Sensors Ltd.), and the torque controller. Each powered exoskeleton joint weighs about 2.9 kg, of which the linear actuator weighs 1.1 kg. The fully detailed mechanical construction, sensor placements, and the torque controller implementation were given in previous work [33].

C. *Human-Exoskeleton Attachment*

In this design, the exoskeleton is attached to the wearer at five main locations, namely, footplate, shank, thigh, pelvis, and torso (Fig. 1). At the footplate, three braces guarantee a firm connection to the shoe of the wearer. At the shank, one brace prevents knee buckling and hyperextension. At the thigh, one brace prevents the human from sliding down out of the pelvis braces due to gravity. The pelvis brace holds the wearer's pelvis in place. Lastly, two backpack braces loosely couple the torso of the wearer with the trunk of the exoskeleton. The footplate and pelvis braces are tight, while the shank and thigh braces are not (four fingers of an adult can be put in when tightened). By doing this, the wearing comfort is improved and unavoidable misalignments between human and exoskeleton joints are tolerated. With cuff-type braces, axial rotations cannot be prevented either, which further tolerates the offset of HEE.

D. *Electronics and Networked Architecture*

Fig. 4 shows the global picture of the exoskeleton network that hosts the lower level control algorithm. The exoskeleton network system makes use of EtherCAT E-Bus as interconnection medium, and EtherCAT fieldbus as the communication medium between the control PC and distributed networked slaves. Using full-duplex structure, all slaves have at least one IN port and one OUT port. Open ports are closed by slave controller automatically. This architecture allows one single cable running through one leg, daisy chaining all slaves. The sampling frequency of the network is 2000Hz.

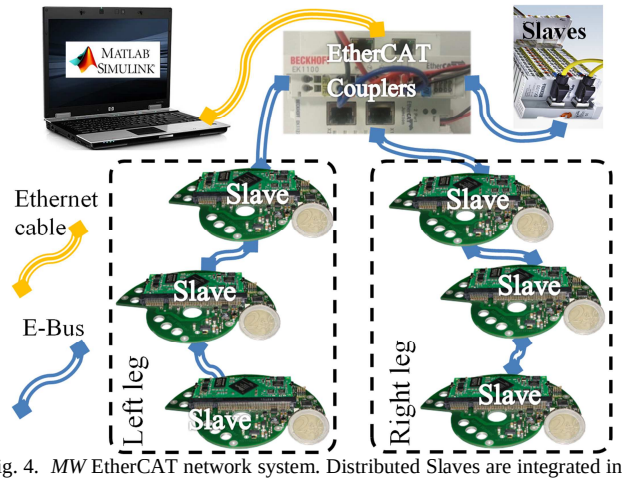

Fig. 4. *MW* EtherCAT network system. Distributed Slaves are integrated in 6 powered DoFs. A PC can communicate with the *MW* network via the onboard EtherCAT Couplers through Ethernet. Extra slaves can be plugged into the EtherCAT Couplers.

This article has been accepted for publication in a future issue of this journal, but has not been fully edited. Content may change prior to final publication. Citation information: DOI 10.1109/TNSRE.2014.2365697, IEEE Transactions on Neural Systems and Rehabilitation Engineering

High-level control update rates are set according to the computing time needed by the control PC.

Six slaves are integrated in the six powered joints. Each slave controls the pulse-width modulation (PWM) sequences of one motor, and allows interfacing with one motor encoder, two analogue-to-digital (ADC) channels, one spring encoder, two joint encoders, one load cell, and one inertial measurement unit (IMU). The motor encoder is responsible for motor commutation, velocity and position control; the ADC channels for roughly measuring the line voltage and temperature of the motor drive; the spring encoder for spring deflection (torque) sensing; two joint encoders for the joint angle of the powered DoF and that of its neighbor passive DoF (e.g., the HEE); the load cell is not used at this moment. On each exoskeleton leg, three IMUs (UM6-LT, CH Robotics LLC) are rigidly attached to the segments, one between HAA and HEE (*lr1*, *ll1*), one at the thigh (*lr3*, *ll3*), and one at the shank (*lr4*, *ll4*). These IMUs provide the absolute orientation of the segments w.r.t. gravity.

E. Design Summary

The current *MW* exoskeleton weights 28kg. It fulfills most of the design requirements specified in Table I-III.

IV. Exoskeleton Control and Operation

The basic control structure consists of three parts, namely:

- a finite-state machine (FSM) that defines different motion scenarios and logics to provide the desired assistance for patients,
- an HMI that can trigger transitions from one state to another in the FSM so that *MW* performs user-intended maneuvers,
- joint-impedance controllers supervised by the FSM to track the desired joint references with variable impedances.

Details are discussed in the following subsections.

A. Finite-State Machine

Part of the FSM is shown in Fig. 5, in which nine states are defined for assisted walking. *Assisted weight shift to left* (S2) and *assisted weight shift to right* (S6) are defined for the active control in the frontal plane, of which the function is to shift the weight of the wearer-exoskeleton to the stance leg. *Half step swings* (S3 and S7) are defined for the gait initiation and termination. The allowed state transitions are depicted in Fig. 6.

B. Human Machine Interface

The *MW* HMI system consists of pushbuttons and a CoM position detection mechanism.

1) Pushbuttons

The wearer or the system operator can use a pushbutton interface to trigger START or STOP walking and stepping.

2) CoM position

A trigger to initiate a step will be generated when the CoM ground projection falls in the desired quadrant.

The CoM position of wearer-exoskeleton is estimated using the IMU mounted on the links (*lr1* or *ll1* in Fig.1) between HAA and HEE, joint angles of HAA, HFE, and KFE (see Fig. 7), in combination with the geometrical and mass properties of the exoskeleton and the human anatomical data from [36].

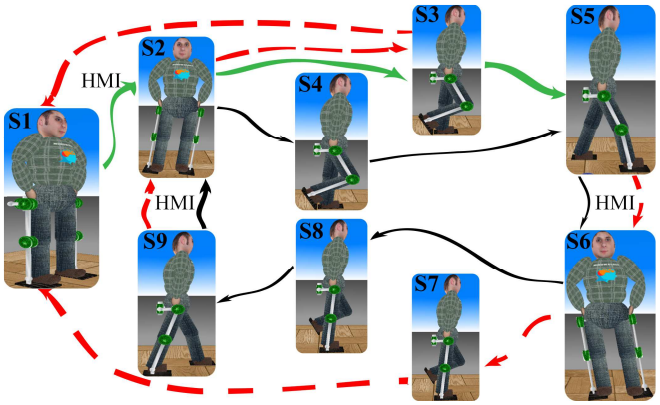

Fig. 5. Finite- state machine for the stance and gait assistance. A full gait cycle is labelled by black solid arrows; gait initiation by green solid arrows; gait termination by red dashed arrows. The states names are:

S1 = *stand*
S2 = *assisted weight shift to left*
S3 = *half step right swing*
S4 = *full step right swing*
S5 = *double stance right foot leading*
S6 = *assisted weight shift to right*
S7 = *half step left swing*
S8 = *full step left swing*
S9 = *double stance left foot leading*

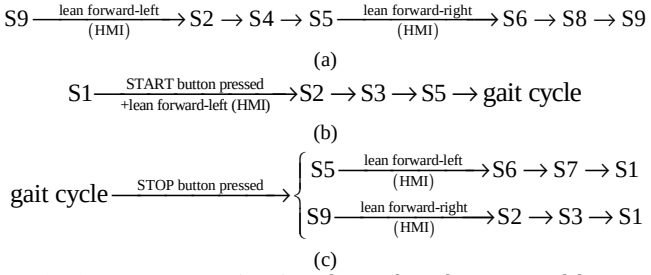

Fig. 6. State transitions. "(HMI)" indicates that other HMI modalities are allowed. Here the trunk motion is used. Arrows without texts indicate that the transitions take place automatically when the previous state is completed. (a) A gait cycle. (b) Gait initiation via a *half swing* (S3). (c) Gait termination. When the STOP button is pressed, the state machine proceeds to the nearest termination state (S9 or S5) and via *half swings* (S3 or S7) returns to *stand* (S1).

To calculate the relative CoM position w.r.t. the leading stance foot, in standing and double stance phase, a sagittal weight shift coefficient r_S (sagittal coef. for short) and a lateral weight shift coefficient r_L (lateral coef.) are defined,

$$r_S = \frac{x_{CoM}}{x_{ADP}},\ r_L = \frac{z_{CoM}}{z_{ADP}} \tag{1}$$

where $x_{CoM}, x_{ADP}, z_{CoM}$ and z_{ADP} are defined in Fig. 7.

These two coefficients normally vary between 0 and 1, and they are evaluated only in state S1, S2, S5, S6, and S9. When the CoM ground projection gets close to the leading stance foot, these values approach 0. When they are both smaller than the predefined thresholds (r_S<0.35 and r_L<0.45), an *assisted weight shift* (S2 or S6) is triggered.

C. Joint Reference Generation and Tracking

1) Joint Position Reference Generation

Reference joint angles for HAA, HFE, and KFE are defined for different states. In stance/double stance (S1, S5, S9), references are defined such that the user is comfortably standing straight. In weight shifting (S2, S6), references are online generated by a smooth interpolation between the end posture of the double stance phase and the beginning of the

This article has been accepted for publication in a future issue of this journal, but has not been fully edited. Content may change prior to final publication. Citation information: DOI 10.1109/TNSRE.2014.2365697, IEEE Transactions on Neural Systems and Rehabilitation Engineering

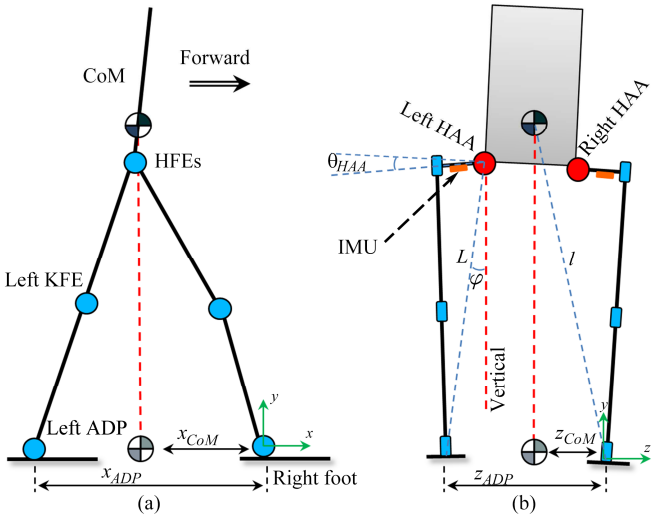

Fig. 7. Sketch of estimating the CoM position. (a) in the sagittal plane and (b) in the frontal plane. x_{CoM} and z_{CoM} are distances between CoM ground projection and the leading (right) foot in the sagittal and frontal plane, respectively. x_{ADP} and z_{ADP} are step length and step width, respectively. L is the distance between the swing HAA and foot. φ is the angle between L and gravity. l is the pendulum length.

swing phase. In swing phases (S3, S4, S7, and S8), references for HFEs and KFEs are based on recorded gait of an unimpaired subject wearing this exoskeleton in zero-torque mode. They are modified to ensure sufficient foot clearance. Five key points in the recorded hip and knee flexion/extension trajectories are manually adjusted and fitted by splines. The fitted curves are smoothed using local regression techniques [37]. References for HAAs are template based and online adapted to improve stability in the frontal plane (see next section).

2) Step-Width Adaptation (SWA)

The foot placement in the frontal plane is online adapted after mid-swing to improve wearer-exoskeleton lateral stability. If the wearer-exoskeleton falls towards one side due to perturbations such as trunk or arm motion, or interactions with other people, the foot placement is adjusted to break the fall, resulting in a wider or narrower step.

According to the XCoM concept [24][26], bipedal gait in single stance (swing) is modeled as a linear inverted pendulum (LIP), i.e. a concentrated mass (m) kept at a constant height by a massless extendable leg. The XCoM position in the frontal plane ζ is defined as

$$\zeta = z_{CoM} + \frac{v_{CoMz}}{\omega_0} \tag{2}$$

where z_{CoM} and v_{CoMz} are the lateral CoM position and velocity, respectively, and $\omega_0=\sqrt{g/l}$ is the eigenfrequency of the pendulum, where l is the pendulum length (Fig. 7) and g gravity.

During normal walking without any perturbation, the XCoM position in a certain period (e.g. mid-swing) varies little and its nominal value can be expressed by z_{CoM}^{nom} and v_{CoMz}^{nom}. When the system is perturbed during the swing phase, the deviation ($\Delta\zeta$) of XCoM position from its nominal value is,

$$\Delta\zeta = \Delta z_{CoM} + \frac{\Delta v_{CoMz}}{\omega_0} = \left(z_{CoM} - z_{CoM}^{nom}\right) + \frac{v_{CoMz} - v_{CoMz}^{nom}}{\omega_0} \tag{3}$$

In (3), the CoM position change can be ignored, since it is usually much smaller compared to the velocity term.

In order to counteract the perturbation such that the XCoM returns to its nominal value just at heel strike, step width is adapted. This is achieved by modifying the HAA angle, i.e., adding $\Delta\theta_d^{HAA}$ to the HAA reference θ_d^{HAA}. The resulted step-width change is equal to the deviation of the XCoM position,

$$\Delta\zeta = L\left(\sin\left(\Delta\theta_d^{HAA} + \varphi\right) - \sin\varphi\right), \tag{4}$$

where L and φ are defined in Fig. 7. The CoM position and velocity in (3) and angle φ in (4) are estimated using onboard IMUs and joint encoders.

Rearrange (4) to obtain $\Delta\theta_d^{HAA}$,

$$\Delta\theta_d^{HAA} = \arcsin\left(\frac{\Delta\zeta}{L} + \sin\varphi\right) - \varphi \tag{5}$$

At each sample, $\Delta\theta_d^{HAA}$ can be computed and added to the nominal trajectory θ_d^{HAA}. This is called continuous step-width adaptation. This algorithm was implemented and experimented, but difficulties existed. Due to the noisy output from the IMU gyroscopes, CoM velocity estimation was contaminated with noise as well, which led to vibrations in the HAA joint. At this moment, we implement a one-time adaptation of the HAA trajectory during swing phase when the averaged XCoM change during mid-swing (40-50 percent of a swing) exceeds a predefined threshold. The averaged XCoM change reads,

$$\overline{\Delta\zeta} = \frac{1}{t_2 - t_1}\int_{t_1}^{t_2}\Delta\zeta \tag{6}$$

where t_1 and t_2 are the start and end of the mid-swing.

The one-time HAA joint angle adaptation $\Delta\theta_d^{HAA}$ is computed at t_2 using (5) by replacing $\Delta\zeta$ with $\overline{\Delta\zeta}$.

3) Reference Tracking

Joint references are tracked using variable impedance control. Joint SEAs are treated as torque sources. As illustrated in Fig. 8, errors between measured joint angles and the references, together with desired impedance values, are fed to the impedance controller. The impedance, for now, a stiffness value (P-gain), differs per state (Table IV). These values were empirically determined. In general, high impedances are applied to ensure accurate foot placement and prevent knee buckling, and low values to absorb impact and improve

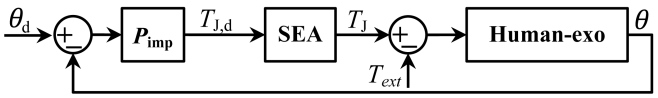

Fig. 8. Impedance-controlled trajectory tracking diagram for a powered joint. Errors between the measured joint angle θ and the reference θ_d, together with desired impedance values, are fed to the impedance controller P_{imp}; the SEA is treated as a torque source; $T_{J,d}$ and T_J are the desired and actual joint torque, respectively. T_{ext} represents all external torques and forces.

TABLE IV
TYPICAL P-GAIN (STIFFNESS) VALUES OF THE IMPEDANCE CONTROLLER

State	Anatomical Plane	Impedance Mode	Stiffness, Nm/rad
S1	Sagittal	Medium	400
	Lateral	Low	50
S2,S6	Sagittal	Medium	400
	Lateral	Medium	500
S3,S4,S7,S8	Sagittal	High	600
	Lateral	High	800
S5,S9	Sagittal &Lateral	High	600

This article has been accepted for publication in a future issue of this journal, but has not been fully edited. Content may change prior to final publication. Citation information: DOI 10.1109/TNSRE.2014.2365697, IEEE Transactions on Neural Systems and Rehabilitation Engineering

wearing comfort. The stiffness of the impedance can vary between 0 and 820 Nm/rad. Damping was set to 0 for these experiments. No oscillation or overshoot was observed in pilot tests. The intrinsic damping (damping of actuators and human joints) proved to be sufficient. There is no need to add additional damping.

V. Evaluation and Results

The proposed CoM position HMI has been tested using walking experiments with four complete SCI paraplegics (males, age 26±11, weight 66±11, injury level T7-T12). In all experiments, pushbuttons were only used to trigger START/ STOP walking. The results are given in Section V.B. and also shown in the multimedia material Scene 1.

We tested the proposed step-width adaption (SWA) algorithm on both paraplegics and healthy subjects. Large disturbances (pushes by a third person) have only been applied to tests with piloting healthy subjects. These results are given in Section V.C and the multimedia material Scene 2-4. The effects of exoskeleton-assisted walking on gait kinetics and EMG patterns are published separately by Sylos-Labini et al. [38].

A. Experiment Setup

All experiments were performed in a laboratory environment, where an 8-meter walkway and double handrails (or crutches) were available. A safety harness worn by the wearer was attached to an overhead suspension system moving along with the wearer, which only came into action when the subject fell. For each subject, each experimental session lasted one-to-two hours. The subject walked 8 meters in a trial. The experiments were performed under the ethical approval given by Comitato Etico Fondazione Santa Lucia.

B. CoM Position as an HMI

In this experiment, the subjects (both healthy and paraplegic subjects) were trained to use their trunk movement to change the wearer-exoskeleton's CoM. Following the instructions about how and when to move their upper body, all subjects managed to learn the techniques in the very beginning of the training session. After one or two trials, they all could repetitively trigger the steps of the exoskeleton on their own.

For example, Fig. 9 illustrates how a SCI subject triggered the state transitions of the FSM. At t=0.25s, the subject started to shift his weight to the front and to the left. At t=0.78s (the first vertical dashed line), both weight-shift coefficients fell below their thresholds, the controller detected the intention of the subject and initiated *assisted weight shift to left* (S2). The *MW* assisted and accelerated the weight shift, as illustrated by the rapid drop in the coefficients after the trigger was given. After the completion of state S2, the state transited automatically to *full step right swing* (S4). Similarly, at t=3.9s, the system detected the user's intention of making a left step and state *assisted weight shift to right* (S6) was triggered. Cyclic gaits were produced in this manner. Weight shift was initiated by the subject, and completed by the exoskeleton.

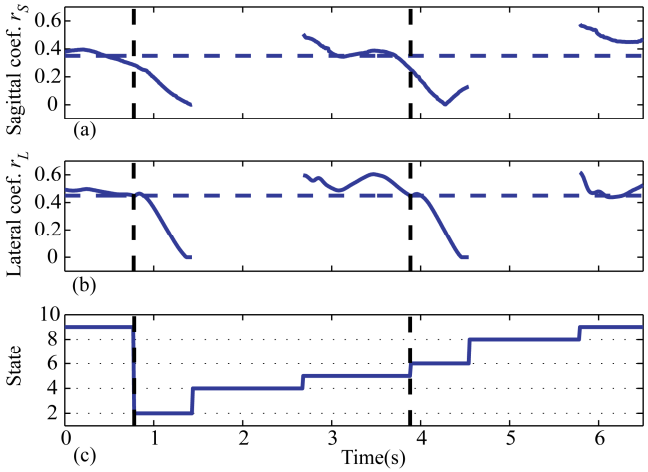

Fig. 9. CoM position triggered exoskeleton stepping by a SCI patient. (a) and (b) show the sagittal and lateral coefficients as a function of time, respectively. When both coefficients are smaller than its thresholds (indicated by the horizontal dashed line), triggers are generated (indicated by a vertical dashed line). (c) shows the corresponding state transitions. A t=0.5s the sagittal coef. r_S first crossed its threshold and then at t= 0.78s, the lateral coef. r_L did. State transited immediately from *double stance left foot leading* (S9) to *assisted weight shift to left* (S2). Similarly, at t=3.9s, due to the user's trunk motion, both coefficients became less than their thresholds, and then the state changed from S5 to S6. In double stance (S2,S6), the coefficients further decreased, meaning, CoM was moved towards the leading stance foot by the exoskeleton.

C. Step-Width Adaptation

The SWA algorithm allowed healthy subjects to walk without external support. SCI subjects still needed the support of handrails. Snapshots of a left step for a healthy subject are shown in Fig. 10. Note: *The subject was carrying the crutches only for safety*.

The SWA algorithm was effective in counteracting disturbances. Fig. 11 illustrates that the algorithm made the step wider to counteract the large change in XCoM position. During the regular left swing (t= [0.5, 1.8] s), the XCoM deviation $\Delta\zeta$ in (4) did not exceed the threshold and nominal joint trajectories were tracked. During the right swing, the subject was pushed and fell quicker to the right. At t = 3.2s, the averaged XCoM deviation exceeded the threshold and the reference HAA angle was online adapted. This resulted in a larger hip abduction at heel strike and a larger step width at t = 3.8s.

For paraplegic subjects, the step width adaption took place, for example, when the subject pulled the handrail with excessive forces, and the measured XCoM deviation exceeded the threshold. The excessive arm forces acted as disturbances, and the exoskeleton reacted in the same way as shown in Fig.

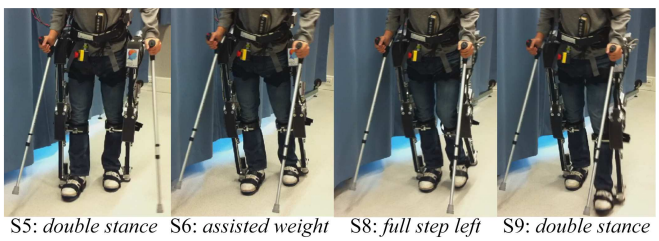

S5: *double stance right foot leading* S6: *assisted weight shift to right* S8: *full step left swing* S9: *double stance left foot leading*

Fig. 10. Snapshots of a left step during straight walking. The crutches were only used for safety and did not touch the ground during the 8-meter walk.

This article has been accepted for publication in a future issue of this journal, but has not been fully edited. Content may change prior to final publication. Citation information: DOI 10.1109/TNSRE.2014.2365697, IEEE Transactions on Neural Systems and Rehabilitation Engineering

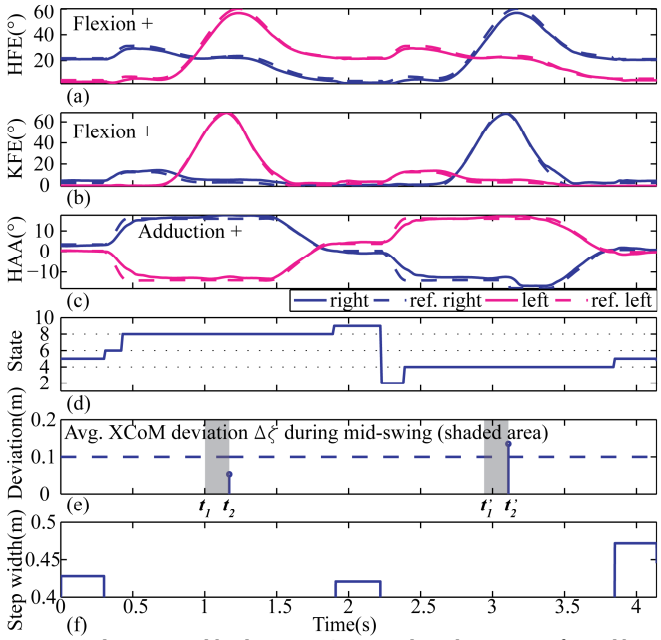

Fig. 11. Online step-width adaptation. A gait cycle with 2 steps performed by a healthy subject using CoM position (trunk motion) as a HMI. (a)(b)(c) are the joint angles. (d) the state. (e) XCoM deviation is accumulated during mid-swing and the time averaged value is computed at t_2 or t_2', shown by the stem plot. The horizontal dashed line indicates the threshold, which is used to determine whether the step width should be adapted. At t=3.2s, the step-width adaptation occurred, due to the excessive perturbation during the right swing. (f) the step width in *double stance* (S5 and S9). The last step became wider compared to previous steps.

11.

After each session, several questions were asked. Walking with and without SWA could be distinguished within several steps. Among different healthy subjects, some reported that the SWA algorithm made their walk more stable and they relied less on crutches. Others reported no difference in terms of gait stability.

VI. Discussion

The goal of this research is to develop a powered exoskeleton to support SCI paraplegics to walk. The *MW* exoskeleton, equipped with compliant series elastic actuators, is able to support SCI patients to walk with support aids. Its actuation capacity and structural strength can deal with subjects weighing up to 100kg. The powered hip ab/adduction allows actively controlled foot placement in the frontal plane. It can also provide assistance in lateral weight shift.

The proposed controllers and human machine interface partially addressed the posture stability and intention-detection issues accompanied with this type of assistive devices. With the current prototype and control implementation, stable walking without crutches is achieved for healthy subjects but not yet for SCI paraplegics. More research and development is needed to further improve the gait stability and let paraplegics walk without support aids.

The current design has some limitations. The total weight of the exoskeleton (28kg) is within the design requirements, but does constrain the portability of this device. We believe that keeping the current linear actuators unchanged, the total weight can be reduced to two thirds by optimizing the structural design. Lack of actuation in some degrees of freedom limits the locomotion capability of the exoskeleton. For example, *MW* does not have powered HEE, which is crucial for active turning. Similarly, *MW* has an unpowered ankle joint, which limits the use of ankle strategy in balance control and the generation of powered push-off during walking.

A. Human Machine Interface

Among the existing exoskeletons, different HMIs have been experimented to determine human intentions and trigger state transitions.

- Manual commands (via pushbuttons/ a joystick) [13][18] and voice commands [14] have been tested. Manual commands are direct expressions of the wearer's/ operator's intention. However, they involve cognitive load and movements, which are not an integral part of locomotion.
- Biosignal-based HMIs, e.g., using brain or muscle activities, have been used for operating a human-augmentation exoskeleton [39] and manipulating an upper limb prosthesis [40], while they have not been applied in SCI gait assistance.
- Currently, most exoskeletons trigger the state transitions by analyzing the data collected by onboard sensors and applying intention detection algorithms [11][13][15]. Our implementation belongs to this category.

For the third category, different body movements and algorithms have been used. In [11], the user triggers the steps of the exoskeleton by leaning forward, detected by a trunk tilt sensor. In [13], the user triggers the steps by a forward arm movement (detected by an IMU on each arm). In [15], stepping is also triggered by leaning forward. CoM ground projection in the sagittal plane, which is computed using data from thigh accelerometers and joint encoders, is used to detect the trunk motion. This is similar to our approach. For the *MW*, the user leans forward as well as sideways to trigger steps, whereas CoM projection in both the sagittal and frontal planes is used. Natural gait is not constrained to the sagittal plane and lateral weight shift is an integral part of gait. We believe that making use of the information in the frontal plane could potentially improve the detection success rate. To compare the effectiveness and robustness of different algorithms, we need to implement them on the same device.

Besides the reported CoM position HMI, we have also tested biosignal-based HMIs using *MW*, e.g., step triggering using arm muscle (anterior portions of deltoid muscles) electromyography (EMG) and using electroencephalogram (EEG) related to steady-state visual evoked potentials (SSVEP). The preliminary experiments are shown in the multimedia material Scene 5-6. Further study will be carried out to compare the performance of different HMIs.

B. Frontal Plane Actuation

Powered hip ab/adduction is critical in supporting lateral balance. Currently most existing exoskeletons only have actuated hip and knee flexion/extension. The wearer has to use

This article has been accepted for publication in a future issue of this journal, but has not been fully edited. Content may change prior to final publication. Citation information: DOI 10.1109/TNSRE.2014.2365697, IEEE Transactions on Neural Systems and Rehabilitation Engineering

crutches to stabilize. Only few exoskeletons included powered HAA (see e.g. [17] and [19]), though no exoskeleton has reported the use of the HAA to actively stabilize gait.

C. Step-Width Adaptation

Most exoskeletons produce gait by tracking fixed and pre-defined joint reference trajectories, generated in various ways [12][14][16][18]. One obvious downside of tracking fixed references is the limited capability of maintaining balance and counteracting disturbances.

In our experiments, the XCoM concept has been applied to adapt the step-width to counteract disturbances during gait. To the authors' knowledge, this is the first exoskeleton that incorporates this concept. Previously, mainly theoretical studies on XCoM have been published [24][26]. The XCoM theory has been verified mainly using human experiments (e.g. [25][41][42]). A closely related concept, the *capture point* theory, is rapidly gaining popularity in the dynamic balance control of humanoids. It has been applied in the control of different humanoids to balance or to recover from pushes [43][44]. Still it has not been applied to exoskeletons.

In our approach, the balance control of the human-exoskeleton combined system is partially addressed. The step-width adaptation algorithm actively makes the steps wider to avoid tipping over. However, we do not know whether the algorithm improved the gait stability during steady-state walking. To access the stability improvement, we have used some indicators such as *margin of stability* (see [45]). But no consistent results have been found. This can be caused by several factors:

- Human factor: The way that the subject perceives and interacts with the exoskeleton and the SWA controller can vary between subjects and even per step for the same subject.
- Accuracy of the XCoM estimation: In the experiments, no sensor has been placed on the human body. The relative motion between the wearer and the exoskeleton can cause estimation error.
- Accuracy of foot placement: The lack of actuation in the ankle joint limits the controllability of the system. Furthermore, though the exoskeleton is equipped with powerful actuators, the interaction forces from wearer's limbs can disturb the exoskeleton and cause errors in the foot placement.

These factors have to be tackled one by one before a consistent conclusion can be made.

D. Series Elastic Actuator

Additionally, it can be argued that the joint controller has not fully made use of the advantages of torque-controllable SEAs. The current implementation is simple and does not involve heavy computations such as inverse kinematics or dynamics. Additionally it works with the XCoM concept directly. However to fully explore the potential of SEAs, a force/ torque-based balance controller (see e.g. [46]-[48]) should be investigated.

ACKNOWLEDGMENT

The authors thank Arthur Ketels (Speciaal Machinefabriek Ketels v.o.f., the Netherlands) for providing the custom-made high power electronics and EtherCAT-technology support. *MINDWALKER* project consortium also greatly appreciates the tremendous effort of all the testing subjects.

REFERENCES

[1] D. M. Dryden, L. D. Saunders, B. H. Rowe, L. A. May, N. Yiannakoulias, L. W. Svenson, D. P. Schopflocher, and D. C. Voaklander, "Utilization of health services following spinal cord injury: a 6-year follow-up study," Spinal Cord, vol. 42, no. 9, pp. 513–525, Jul. 2004.

[2] M. Wyndaele and J-J. Wyndaele, "Incidence, prevalence and epidemiology of spinal cord injury: what learns a worldwide literature survey?" Spinal Cord, vol. 44, no. 9, pp. 523-529, Jan. 2006.

[3] J. L. Collinger et al., "Functional priorities, assistive technology, and brain-computer interfaces after spinal cord injury." Journal of Rehabilitation Research and Development, vol. 50, no. 2, pp. 145-160, Apr. 2013.

[4] M. Massucci, G. Brunetti, R. Piperno, L. Betti, M. Franceschini, "Walking with the Advanced Reciprocating Gait Orthosis (ARGO) in thoracic paraplegic patients: energy expenditure and cardiorespiratory performance," Spinal Cord, vol. 36, no. 4, pp. 223-227, 1998.

[5] G. Scivoletto, A. Petrelli, L.D. Lucente, A. Giannantoni, U. Fuoco, F. D'Ambrosio, and V. Filippini, "One year follow up of spinal cord injury patients using a reciprocating gait orthosis: preliminary report." Spinal Cord, vol. 38, no. 9, pp. 555-558, Sep. 2000.

[6] G. Scivoletto, M. Mancini, E. Fiorelli, B. Morganti and M. Molinari, "A prototype of an adjustable advanced reciprocating gait orthosis (ARGO) for spinal cord injury (SCI)," Spinal Cord, vol. 41, no. 3, pp. 187-191, Mar. 2003.

[7] M.K. Vukobratovic, "When were active exoskeletons actually born?" Inter. J. of Humanoid Robotics, vol. 4, no. 3, pp. 459-486, Jan. 2007.

[8] A. B. Zoss, H. Kazerooni, A. Chu, Biomechanical Design of the Berkeley Lower Extremity Exoskeleton (BLEEX), IEEE/ASME Trans. on Mechatronics, vol. 11, no. 22, pp. 128-138, Apr. 2006.

[9] K. Kong, D. Jeon, "Design and control of an exoskeleton for the elderly and patients," IEEE/ASME Trans. on Mechatronics, vol. 11, no. 4, pp. 428-432, Aug. 2006.

[10] Gait-Locomotor Apparatus, by A. Goffer. (2002, Nov. 27). WIPO Patent EP 1260201
[Online]. Available: WIPO: HOME: IP Services: PATENTSCOPE

[11] Locomotion Assisting Device and Method, by A. Goffer and C. Zilberstein. (2013, May 16). US Patent, US 20130123672 A1
[Online]. Available: WIPO: HOME: IP Services: PATENTSCOPE

[12] T.A. Swift, "Control and Trajectory Generation of a Wearable Mobility Exoskeleton for Spinal Cord Injury Patients," Ph.D. dissertation, Dept. Mech. Eng., Univ. of California, Berkeley, CA, 2011.

[13] Human Machine Interface For Human Exoskeleton, by R. Angold, J. Burns, D. Fairbanks, N. Harding, H. Kazerooni, K. Strausser, T. Swift, and A. Zoss. (2012, Mar. 22), WIPO patent, WO2012037555A1
[Online]. Available: WIPO: HOME: IP Services: PATENTSCOPE

[14] R. J. Farris, et al., "Preliminary Evaluation of a Powered Lower Limb Orthosis to Aid Walking in Paraplegic Individuals." IEEE Transactions on Neural Systems and Rehabilitation Engineering, vol. 19, no. 6, pp. 652-659, Oct. 2011.

[15] H. A. Quintero, et al., Control and implementation of a powered lower limb orthosis to aid walking in paraplegic individuals. IEEE Int. Conf. on Rehab. Robotics (ICORR), 2011

[16] P. D. Neuhaus, J. H. Noorden, T. J. Craig, T. Torres, J. Kirschbaum, J.E. Pratt, "Design and evaluation of Mina: A robotic orthosis for paraplegics," IEEE Int. Conf. on Rehab. Robotics, 2011.

[17] Mobility Aid, by R. Little and R. A. Irving. (2009, Jul. 2). WIPO Patent, WO 2009082249 A2
[Online]. Available: WIPO: HOME: IP Services: PATENTSCOPE

[18] Control System for a Mobility Aid, by F. Almesfer and A. J. Grimmer. (2011, Jan. 6). WIPO Patent, WO 2011002306 A1
[Online]. Available: WIPO: HOME: IP Services: PATENTSCOPE

This article has been accepted for publication in a future issue of this journal, but has not been fully edited. Content may change prior to final publication. Citation information: DOI 10.1109/TNSRE.2014.2365697, IEEE Transactions on Neural Systems and Rehabilitation Engineering

[19] H. K. Kwa, J. H. Noorden, M. Missel, T. Craig, J. E. Pratt, P. D. Neuhaus, Development of the IHMC mobility assist exoskeleton, IEEE Int. Conf. on Robot. and Auto., Kobe, Japan, 2009.
[20] T. McGeer. "Passive dynamic walking." International Journal of Robotics Research, vol. 9, no. 2, pp. 62-82, Apr. 1990.
[21] A. Kuo, "Stabilization of lateral motion in passive dynamic walking," International Journal of Robotics Research, vol. 18, no. 9, pp. 917–930, 1999.
[22] J. M. Donelan et al., "Mechanical and metabolic requirements for active lateral stabilization in human walking," Journal of Biomechanics, vol. 37, no. 6, pp. 827-835, Jun. 2004.
[23] C. E. Bauby and A. D. Kuo, "Active control of lateral balance in human walking," Journal of Biomechanics, vol. 33, no. 11, pp. 1433-1440, Nov. 2000.
[24] A. L. Hof, "The 'extrapolated center of mass' concept suggests a simple control of balance in walking." Human Movement Science, vol. 27, no. 1, pp. 112-125, Feb. 2008.
[25] A. L. Hof and J. Duysens, "Responses of human hip abductor muscles to lateral balance perturbations during walking." Experimental Brain Research, vol. 230, no. 3, pp. 301-310, Aug. 2013.
[26] A. L. Hof et al., "The condition for dynamic stability." Journal of Biomechanics, vol. 38, no. 1, pp. 1-8, Jan. 2005.
[27] D. Scholz, S. Kurowski, K. Radkhah, O. von Stryk, "Bio-inspired motion control of the musculoskeletal BioBiped1 robot based on a learned inverse dynamics model," 11th IEEE-RAS Int. Conf. on Humanoid Robots (HUMANOIDS), Oct. 2011.
[28] N. Hogan, "Adaptive control of mechanical impedance by coactivation of antagonist muscles," IEEE Trans. on Automatic Control, vol. 29, no. 8, pp. 681-690, Aug. 1984.
[29] J. E. Pratt and B. T. Krupp. Series elastic actuators for legged robots. Proceedings of SPIE - The International Society for Optical Engineering. 2004.
[30] R. C. Browning, J. R. Modica, R. Kram, A. Goswami, "The effects of adding mass to the legs on the energetics and biomechanics of walking," Med. Sci. Sports Exerc., vol. 39, no. 3, pp. 515-525, Mar. 2007.
[31] S. Wang, W. van Dijk, H. van der Kooij, "Spring uses in exoskeleton actuation design," IEEE Int. Conf. on Rehab. Robotics, Zurich, Switzerland, 2011
[32] K. Shamaei et al. "Estimation of Quasi-Stiffness of the Human Hip in the Stance Phase of Walking." PLoS ONE, vol. 8, no. 12, e81841, 2013
[33] S. Wang, C. Meijneke, and H. van der Kooij, "Modeling, Design, and Optimization of Mindwalker Series Elastic Joint," Int. Conf. on Rehabilitation Robotics, Jun 2013
[34] A.H.A. Stienen, E.E.G. Hekman, H. ter Braak, A. M. M. Aalsma, F. C. T. van der Helm, and H. van der Kooij, "Design of a Rotational Hydroelastic Actuator for a Powered Exoskeleton for Upper Limb Rehabilitation", IEEE Trans. on Biomedical Eng., vol. 57, no. 3, pp. 728-725, Mar. 2010.
[35] C. Lagoda et al. Design of an electric series elastic actuated joint for robotic gait rehabilitation training. 3rd IEEE RAS/EMBS Int. Conf. on Biomedical Robotics and Biomechatronics (BioRob), 2010.
[36] D. A. Winter, "Biomechanics and Motor Control of Human Movement," 4th ed. John Wiley & Sons, Inc. New Jersey, 2009.
[37] W. S. Cleveland, "Robust Locally Weighted Regression and Smoothing Scatterplots." Journal of the American Statistical Association, vol. 74, no. 368, pp. 829-836. 1979.
[38] F. Sylos-Labini et al., "EMG patterns during assisted walking in the exoskeleton." Frontiers in Human Neuroscience, vol. 8, no. 423, Jun. 2014.
[39] Cyberdyne Inc. retrieved in Aug. 2013, http://www.cyberdyne.jp/english/
[40] L. Hochberg et.al., "Neuronal ensemble control of prosthetic devices by a human with tetraplegia," Nature, vol. 442, no. 7099, pp. 164-171, Jul. 2006.
[41] A. Hof, R. van Bockel, T. Schoppen, and K. Postema, "Control of lateral balance in walking: Experimental findings in normal subjects and above-knee amputees," Gait and Posture, vol. 25, no. 2, pp. 250-258, Feb. 2007.
[42] L. Hak et al., "Steps to Take to Enhance Gait Stability: The Effect of Stride Frequency, Stride Length, and Walking Speed on Local Dynamic Stability and Margins of Stability," PLoS ONE, vol. 8 no. 12, e82842, Dec. 2013.
[43] J. Pratt, J. Carff, S. Drakunov, and A. Goswami, "Capture Point: A Step toward Humanoid Push Recovery." IEEE-RAS Int. Conf. Humanoid Robots, pp. 200-207, Dec. 2006.
[44] T. de Boer, "Foot placement in robotic bipedal locomotion," Ph.D. dissertation, Biomech. Eng. Dept., Delft Univ. of Tech., Delft, the Netherlands, 2012.
[45] A. L. Hof et al., "The condition for dynamic stability." Journal of Biomechanics 38(1): 1-8. 2005.
[46] B. J. Stephens and C. G. Atkeson. Dynamic Balance Force Control for compliant humanoid robots, Intelligent Robots and Systems (IROS), 2010 IEEE/RSJ International Conference on. 2010.
[47] C. Ott et al. Posture and balance control for biped robots based on contact force optimization, Humanoid Robots (Humanoids), 11th IEEE-RAS International Conference on. 2011.
[48] R. Ozawa, and J. Ishizaki. Passivity-based symmetric posture control and the effects of mass distribution and internal impedance on balance. Humanoid Robots (Humanoids), 12th IEEE-RAS International Conference on. 2012.

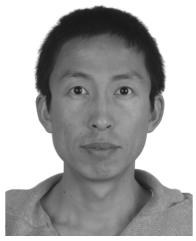

Shiqian Wang received a B.S. degree in mechanical engineering from Harbin Institute of Technology, Harbin, China, in 2007 and an M.Sc. degree in control system technology from Eindhoven University of Technology, Eindhoven, the Netherlands, in 2009. He is pursuing a Ph.D. degree in biomechanical engineering at Delft University of Technology, the Netherlands.

His research interests include the development of wearable robots such as orthotic or prosthetic devices.

Mr. Wang's awards and honors include Zengxianzi Scholarship, cum laude undergraduate, ASML Scholarship, nominated top-10 best student paper awards in ICORR 2013.

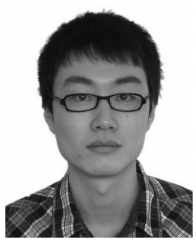

Letian Wang was born in Yan'an, China, in 1984. He received a B.S. degree in mechanical engineering from Shanghai Jiao Tong University, Shanghai, China, in 2007, and an M.Sc. degree in systems and control engineering from Delft University of Technology, Delft, the Netherlands, in 2009. He is pursuing a Ph.D. degree at University of Twente, Enschede, the Netherlands.

His current research interests include robot control-system design, bipedal locomotion generation, and human-in-the-loop simulations.